Precise Measurement of Physical Activities and High-Impact Motion: Feasibility of Smart Activity Sensor System

Hung-Ping Liu, Yu-Min Chuang, Chih-Hao Liu, Phillip C. Yang, and Chiou-Shann Fuh, *Member, IEEE*

***Abstract*—Today, over 72% of the world-wide population lives beyond the age of 65. Senior care has become one of the single most relevant challenges globally. There are many relevant issues related to monitoring and managing the daily activities of senior citizens. In this study, we will examine the role of advanced activity sensor platform to monitor their daily activity levels. It will assist in understanding the lifestyle of the individual seniors to promote safety and improve the quality of life through measurement of physical strength and independence. We investigate the requirements of wearable technology for the seniors, employing Inertial Measurement Unit (IMU) sensor for senior care. The proposed system includes a wearable device for each senior, Internet of Thing (IoT) receiver environment, smart alert, and cloud-based machine learning algorithm with Application Processing Interface (API) enabled remote Internet access. The primary application of our proposed IMU sensor application includes precise measurement of individual physical activity level.**

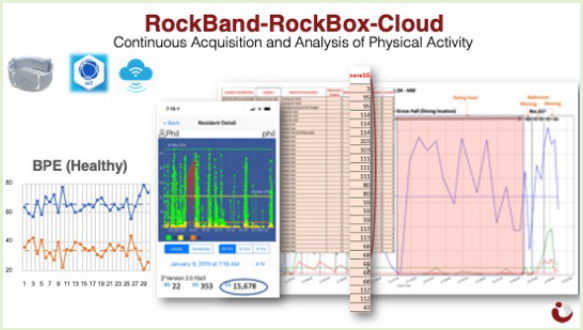

***Index Terms*—Smart sensor, wearable technology, fall detection, activity percentage, physical activity.**

I. Introduction

THE advances in medical care is prolonging the average human longevity world-wide. More people are living beyond 65 years of age [4]. According to the United States Department of Health and Human Services (HHS), the population of the elders over the age of 65 number 49.2 million in 2016 (the most recent year for which data are available). They represent 15.2% of the population, about one in every seven Americans. The number of older Americans increase by 12.1 million or 33% since 2006, compared with an increase of 5% for the under-65 population [1]. Senior care is emerging as an increasingly important topic. The senior lifecare services include the following: a) residential care, consisting of skilled nursing facility, assisted living and independent living homes and b) non-residential care, consisting of home healthcare, adult day care, and hospice [18]. More than one fourth of people over 65 years fall each year [6]. According to the US National Security Council, the number of seniors over 65 who are directly or indirectly killed by a fall ranked first, reaching 33% of the total numbers of accidental deaths in this age group. Zhu *et al.* [19] did a survey of fall detection algorithm for elder. They categorized the identification methods of human falls into two kinds devices: wearable and non-wearable detection devices. Wearable detection devices are based on accelerometer or combined sensors. Non-wearable detection devices are based on sound or video cues.

The wearable technology started in a form of a basic watch worn by people to tell time. The modern wearable technology evolved with ubiquitous computing, miniaturized sensors, and wearable computer technology. Fitbit released its first wearable watch around 2009 and focused on activity tracking. During the ensuing years, smartwatches became common technology products by the electronics companies. These developments led to Gemperle *et al.* [12] to propose a set of design guidelines for wearability and wearable forms. After considering various

Manuscript received July 1, 2020; accepted July 21, 2020. Date of publication August 10, 2020; date of current version December 4, 2020. This work was supported in part by the Test Research, in part by the Jorjin Technologies, in part by the PowerShow Ltd. (PSL), in part by the Egistec, in part by the D8AI, in part by the LuxVisions Innovation (LVI), and in part by the AiCare Ltd. The associate editor coordinating the review of this article and approving it for publication was Dr. Edward Sazonov. *(Phillip C. Yang and Chiou-Shann Fuh are co-senior authors.) (Corresponding author: Hung-Ping Liu.)*

Hung-Ping Liu is with the Graduate Institute of Biomedical Electronics and Bioinformatics, National Taiwan University, Taipei 10617, Taiwan (e-mail: howardliu1223@gmail.com).

Yu-Min Chuang is with Losheng Sanatorium, Ministry of Health and Welfare, New Taipei City 242, Taiwan, also with Ten-Chan General Hospital (TCGH), Taoyuan 320, Taiwan, and also with the Medical School, National Yang-Ming University, Taipei 112, Taiwan (e-mail: erictpe28@gmail.com).

Chih-Hao Liu is with AiCare, Inc., San Jose, CA 95134 USA (e-mail: alvin.liu@aicare.co).

Phillip C. Yang is with AiCare, Inc., San Jose, CA 95134 USA, and also with the Department of Medicine (Cardiovascular Medicine), School of Medicine, Stanford University, Stanford, CA 94305 USA (e-mail: phillip.yang@aicare.co).

Chiou-Shann Fuh is with the Department of Computer Science and Information engineering, National Taiwan University, Taipei 10617, Taiwan (e-mail: fuh@csie.ntu.edu.tw).

Digital Object Identifier 10.1109/JSEN.2020.3015392

functionalities and requirements, the wrist band offered the most practical and compliant design solution to the seniors.

However, the wearable technology for the elders should embody different applications and designs specific to their usage. In this manuscript, we will demonstrate these specifications in more detail. We will present AiCare's comprehensive technology solution, consisting of wearable sensor, BLE-enabled IOT infrastructure, machine learning algorithm to implement artificial intelligence, and API-enabled web technology to measure daily activities of senior citizens. In developing this technological infrastructure for senior citizens, there were major considerations.

A. Wireless Protocol

Considerations for the requirements of data collection, long-term use, power consumption, wireless transmission distance, legal radio frequency, home use, popularity, and cost lead to the Bluetooth Low Energy (BLE) as the optimal protocol for long term senior care indoor usage.

B. Identification

The personalized data are anonymized using an internally specified identification (ID) system for data collection. BLE Media Access Control (MAC) address for each individual band enables this functionality.

C. Battery Replacement or Power Charge

The senior citizens must be wearing the battery powered smart band at all times. It is impractical for the seniors to remove the smart band for a long period of time or with high frequency as they will not be monitored for data collection during this duration. The time required to charge the batteries is much longer than the time needed to replace the batteries, thus our smart band does not use rechargeable battery. At least 45 days of continuous use is possible with AiCare wrist sensor. AiCare wrist sensor uses battery of Toshiba CR2450 3.0V 620 mAh, power consumption of off: 0.14 mA and normal run: 0.355 mA, thus average continuous run: 52 days.

D. Alert Service

It is important for the seniors to be able to access the alert service easily. Traditionally, many alert service bells are installed throughout the nursing home where they can activate readily in many places that require special assistance such as the bath room and toilet. The BLE protocol will easily provide this service. The smart band could feature a readily accessible button for alert service in an emergency while it is inaccessible during the normal activities. They should be able to activate the alert service from any indoor location.

E. Real-Time Location

There have been many technical developments to address this functionality. The Received Signal Strength Indication (RSSI) is used to infer the indoor device location. Jianyong *et al.* [38] proposed a set of tools for this purpose: 1) Gaussian filter to pre-process the received signal, 2) distance weighted filter to reduce the influence of abnormal RSSI, 3) collaborative localization algorithm based on Taylor series, 4) expansion method, and 5) active learning of BLE reference nodes. Their experiments showed that the location tracking accuracy with a margin of error of less than 1.5 meters to be higher than 80%.

Kajioka *et al.* [27] did an indoor position experiment based on RSSI of BLE beacon. By applying their estimation method, they achieved over 95% correct estimation rate with an accurate tracking inside or outside a room. The degradation of a correct estimation rate is possibly due to radio influence issues such as multipath, reflection, or interference.

Rida *et al.* [23] proposed Trilateration algorithm, which can be easily implemented with hardware due to its low complexity. Their approach is based on the deployment of equidistant nodes on the ceiling and each node broadcasts a periodic beacon at a time interval of 400ms. Their proposed method has about $0.5 \sim 1$ meters of error on average.

F. Fall Detection

Lindemann *et al.* [36] proposed an algorithm based on a hearing-aid tool which included an accelerometer and was fixed behind the ear. They demonstrated that their proposed method in the head is better than other fall detectors worn at the hip or wrist.

Wang *et al.* [8] reported an algorithm in which the sensor is also placed on the head. Their proposed method could distinguish eight types of fall and seven daily activities.

Sorvala *et al.* [2] demonstrated a two-threshold algorithm for fall detection. The algorithm combined triaxial accelerometer and triaxial gyroscope data measured from the waist. They could distinguish between fall, possible fall, and activity of daily living. The sensitivity is 95.6% and the specificity is 99.6%. Khojasteh *et al.* [26] also used a threshold-based solution to detect a fall.

Vavoulas *et al.* [14] provided a MobiFall dataset that recorded human activities using accelerometer and gyroscope from smartphone. The activities included four different falls and nine different activities of daily living. Vallabh *et al.* [25] used this dataset to do fall detection by machine learning algorithm. They discovered that K-Nearest Neighbors' (KNN) algorithm is the best approach out of the five different classification methods. Mauldin *et al.* [35] used a deep learning method to detect a fall.

Lim *et al.* [10] proposed a fall-detection algorithm that combines a simple threshold method and hidden Markov model (HMM) using 3-axis acceleration. The best fall detection, combining the simple threshold and HMM, demonstrated sensitivity, specificity, and accuracy of 99%.

Pierleoni *et al.* [24] proposed a fall detection algorithm that fuses triaxial accelerometer, gyroscope, and magnetometer in a wearable sensor on the waist of the subject.

Casilari *et al.* [11] provided an UMAFall dataset, which incorporated five wearable sensing points located on five different points of the body of the participants.

Finally, Hossain *et al.* [13], [28] proposed a real-time fall detection, using a single 3D commercial accelerometer and

TABLE I
THE COMPARISONS OF EACH FALL DETECTION METHODS

Algorithm	Sensor	Position	Sensitivity	Specificity	Accuracy	Method
Sorvala et al. [2]	accelerometer gyroscope	waist	95.60%	99.60%		thresholds
Lindemann et al. [36]	accelerometer	ear	100.00%			feature extraction based
Wang et al. [8]	accelerometer	head				thresholds
Khojasteh et al. [26]	accelerometer	wrist	83.33%~ 100.00%	80.13%~ 95.62%	80.91%~ 95.15%	feature extraction based + NN, DT, RBS or SVM
Vallabh et al. [25]	accelerometer gyroscope (+orientation data)	trouser pocket	90.70%	83.78%	87.50%	machine learning + KNN
Mauldin et al. [35]	accelerometer	wrist	64.00%	86.00%	70.00%	deep learning
Lim et al. [10]	accelerometer	chest	99.17%	99.69%	99.50%	threshold + HMM
Pierleoni et al. [24]	accelerometer gyroscope magnetometer	waist	90.37%/100%	80.74%/100%	100%/100%	thresholds
Hossain et al. [13, 28]	accelerometer	chest	94.50%	98.40%	97.50%	SVMLA
Our proposed method	accelerometer	wrist	100.00%	99.75%	99.75%	feature extraction based

Support Vector Machine Learning Algorithm (SVMLA). The sensor was placed on the chest.

In a situation of long-term monitoring, battery power consumption must be minimized. Only limited datasets can be collected from a pre-specified environment. We, therefore, propose a fall detection method, employing use-pattern recognition by state machine detection with high sensitivity, specificity, and accuracy with low-power consumption. Table I shows the comparisons of each fall detection methods.

G. Physical Activity

Physical activity is defined as any bodily movement produced by skeletal muscles that results in energy expenditure [7]. It is difficult to directly measure physical activity. It requires a dedicated laboratory to measure and perform a kinematic analysis. The measurement period is also short and hard to monitor all day. Wearable technology and wireless data transmission facilitate long-term assessment of physical activity.

Steele *et al.* [3] showed that a triaxial movement sensor was a reliable, valid, and stable measurement of walking and daily physical activity in COPD (Chronic Obstructive Pulmonary Disease) patients.

Yang and Hsu [5] proposed a portable system for physical activity assessment in a home environment. Their proposed system provides significant information in evaluation of health and the quality of life of subjects with limited mobility and chronic diseases.

Diaz *et al.* [17] demonstrated that the estimates of step count and energy expenditure are strongly correlated with observed step counts and measured energy expenditure using the hip- and wrist-based Fitbit® devices.

Finally, Ahmad *et al.* [20], [22] used walk accelerator data and gait raw data for user identification, but did not explain how to identify the walk activity in daily activity. We could use their methods to identify the users by their weekly physical activity in the future.

In this study, we proposed an assessment of the physical activity by triaxial accelerometer, which provides the optimal solution between technological complexity and reliable measurement of physical activity. The assessment of physical activity can help to evaluate the behavior changed by some prescriptions and reinforce the fall detection.

H. Statistics and Artificial Intelligence

The data quantity correlates with the detailed measurement of the seniors' daily activities. We can assess their quality of life through accurate measurements of their activities while they are awake, performing various activities of daily living, participating in activities, and resting. We can also locate their active area indoor, the most frequented area, and duration of stay in each area. We can use their first week data for baseline training data analysis. Subsequently, we can analyze the trend during the ensuing months to detect the significant changes in their activity level. Multiple layers of big data analytics [16], data mining algorithms [37], and machine learning (artificial intelligence) methods are employed [9].

I. AiCare Platform

AiCare platform enabled data collection and real-time analysis are described here. This proprietary platform includes wearable sensor for each senior, IoT and BLE infrastructure, and backend cloud-based system with secure redundant database, machine learning artificial intelligence algorithms, and

(a) RockBand.

(b) RockBox (Raspberry Pi 4 with our custom-designed software).

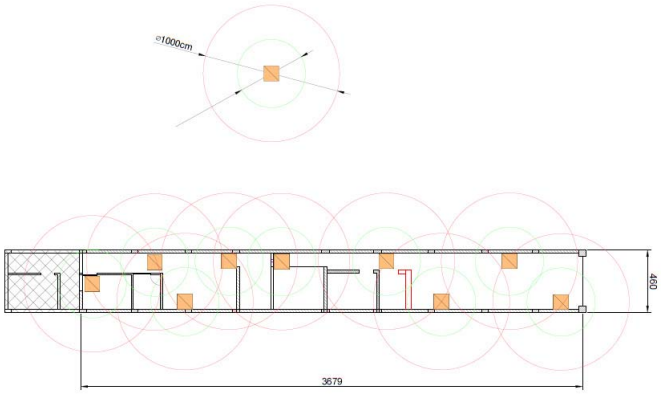

(c) Installation and coverage of RockBoxes in the rooms. An orange box designates a RockBox.

Fig. 1. The picture of RockBand, RockBox, and the installation of RockBoxes in the rooms.

API-enabled internet system. This comprehensive platform is utilized to analyze the seniors' activity data. This service empowers a smart, safe, and secure environment. Their real-time, intelligent system enables timely tracking, detection and prevention to promote healthy and independent senior life.

II. Data Collection and Analysis

A. Fall Detection

We use AiCare's wristband sensor, RockBand™ (RB) as in Fig. 1(a), and RockBox as in Fig. 1(b) for data collection. Fig. 1(c) is the installation and coverage of RockBoxes in the rooms. We record 12 different simulated falls and each simulated fall with 3 repeats. Falls include forward, backward, leftward and rightward with band in left and right hand

Fig. 2. Continued pictures of a fall. (An example of fall type 3).

TABLE II
Types of Fall

Number	Fall Type	Number	Fall Type
1	Forward (left hand)	7	Leftward (right hand)
2	Backward (left hand)	8	Rightward (right hand)
3	Leftward (left hand)	9	Slip-type (left hand)
4	Rightward (left hand)	10	Trip-type (left hand)
5	Forward (right hand)	11	Step-down-type (left hand)
6	Backward (right hand)	12	Forced-rotation-type (left hand)

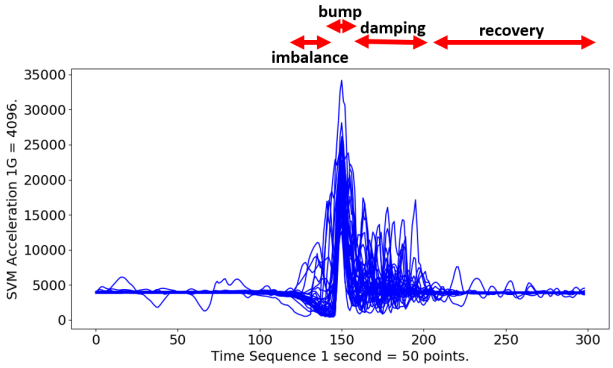

Fig. 3. The SVM of the simulated falls and four phases of the fall pattern.

(8 types) and plus slip-type, trip-type, step-down-type, and forced-rotation-type (4 types) which are shown in Table II. Fig. 2 shows continued pictures of a fall. We use Sum of Vector Magnitude (SVM) to perform the analysis. The SVM is not influenced by wearing the sensor on either the left or right hand. The differences in the initial condition can be removed. The raw data in x, y, and z axes change by rotation of the band, requiring a large data set for different initialization. We only use triaxial accelerometer and no gyroscope due to high power consumption. We propose a simple method to detect a fall. The sample rate is 50 Hz, thus no overlap of data points. The maximum acceleration is $+8$ g or -8 g. Plus or minus means the direction of acceleration toward or far away from the earth. The sensor is 16-bit data, which means 2^{15} is approximately equal to 8 g (8 g $=$ 32768 levels), which calculates to 1 g $=$ 4096 levels. Fig. 3 shows 36 different falls using SVM data. We do moving average with a window $=$ 4 and we align the maximum value of SVM at x position $=$ 250.

From the falls, we separate the fall pattern into 4 phases: imbalance, bump, damping, and recovery. When a senior citizen starts a fall, his or her body cannot be in a proper balance. He or she will move towards the ground. This behavior decreases the gravity of the accelerometer. When the accelerometer sensor stays still, the SVM will be one

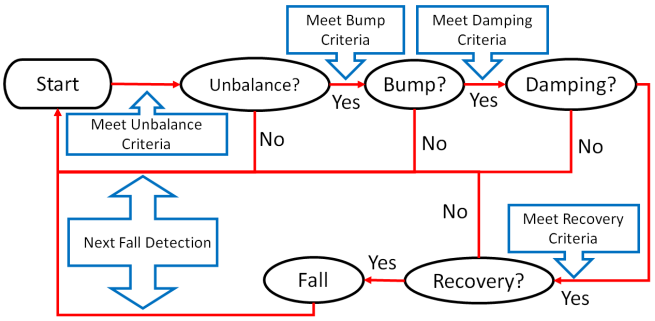

Fig. 4. The state machine of fall detection.

gravity. When the sensor moves to the ground, the SVM of the sensor will decrease relatively. We call this phase the imbalance phase where the bodies of the sensors are in an imbalanced condition. After a short period, he or she will hit the ground. From Fig. 2, we can observe that the period from the initial decrease in SVM to the smallest value is about 0.5 second. When the subject hits the ground, the SVM will reach a maximum during this period of fall. We define the peak period as the bump phase. The peak period is defined as the duration of the maximum SVM of this fall plus left rising edge and right falling edge. After the bump phase, the sensor will be in the damping phase. The seniors will transit from the impact to no motion. The amplitude of SVM will converge back to one gravity during this damping phase. We can observe that the period of damping phase is about 1 second. After the seniors fall back to motionless state, they need some time to recover. We call this the recovery phase where the seniors remain in motionless condition.

We use pattern recognition to detect a fall using four phases of a fall. When we observe a period of SVM, this pattern starts from imbalance and moves sequentially to bump, damping, and recovery phases. These 4 distinct stages are employed to label this behavior as a fall. This is followed by a check, which functions like a state machine where we will check whether the data will meet the criteria of imbalance phase. If this holds true, RB may enter bump phase and proceed to the damping and recovery phases. Fig. 4 shows the detection method.

In the following section, we will demonstrate the mathematic definition of these four phases:

a) Imbalance phase

There are two parameters for this phase: the level and the period.

$$SVM = \sqrt{a_x^2 + a_y^2 + a_z^2} \tag{1}$$

$$SVM < Level_{unbalance} \tag{2}$$

$$t_1 > Period_{unbalance} \tag{3}$$

a_x, a_y, and a_z: the values from the accelerometer for triaxial acceleration.

$Level_{unbalance}$: level threshold of SVM $\sim {}^1\!/_2 g$.

$Period_{unbalance}$: time threshold $\sim$ 200 ms.

t_1 : continuous period of SVM $< Level_{unbalance}$.

When Eqs. (2) and (3) hold, the state will move to imbalance phase. The algorithm will check the bump criteria.

b) Bump phase

There are three parameters for this phase: one level and two periods.

$$SVM > Level_{bump} \tag{4}$$

$$t_2 < Period_{bump\ left\ rising} \tag{5}$$

$$t_3 < Period_{bump\ right\ falling} \tag{6}$$

$Level_{bump}$: level threshold of SVM $\sim 3g$.

$Period_{bump\ left\ rising}$: time threshold $\sim$ 200 ms.

$Period_{bump\ right\ falling}$: time threshold $\sim$ 100 ms.

t_2 : the period of the rising edge to the maximum SVM.

t_3 : the period of the maximum SVM to the falling edge.

c) Damping phase

There are two parameters for this phase: level and period.

$$SVM < Level_{maximum\ SVM\ of\ this fall} \tag{7}$$

$$t_4 = Period_{damping} \tag{8}$$

$Level_{maximum\ SVM\ of\ this\ fall}$: the maximum SVM of this fall.

All the SVMs of the damping phase should be smaller than $Level_{maximum\ SVM\ of\ this\ fall}$.

$Period_{damping}$: define the period of the damping phase $\sim$ 1 second.

t_4 : the period of the damping phase.

d) Recovery phase

There are three parameters for this phase: one level percentage of one gravity and two time periods.

$$1g - p_1 < SVM < 1g + p_1 \tag{9}$$

$$t_5 = Period_{recovery} \tag{10}$$

$$t_6 > Period_{still} \tag{11}$$

p_1 : the percent of $1g$ something like 10%.

$Period_{recovery}$: recovery phase $\sim$ 20 seconds.

$Period_{still}$: still phase $\sim$ 10 seconds.

t_5 : recovery phase.

t_6 : the continuation of SVMs according to Eq. (9) in t_5.

As in Fig. 4, we use state machine method to judge if the state should be entered into the next phase or be back to the initial state. The judgement criteria are the definitions of each phase. For example, to check if the state is entered into the imbalance phase, we will check the g value is smaller than 0.5 g and the period is over 200 ms. If the g value is larger than 0.5 g and the period is smaller than 200 ms, the state is still in the initial state. Otherwise, the state will be entered into the imbalance state. We will check the next criteria of the next phase. We do not use the same phase recognition algorithm for these 4 phases.

Table III shows the percentage of fall types, which demonstrate the features. These 4 features can detect a fall reliably.

We do not use machine learning method in fall detection. Two reasons for not using machine learning method in fall detection: 1) power consumption: our hardware cannot run machine learning algorithm. We even do not use the gyro data for fall detection. The power consumption of gyro is about six times of the g sensor. 2) data sets: we do not have enough simulated data sets to do machine learning. We can use search method to find the maximum and minimum threshold. We will use these thresholds to remove some false alarms. If we can

TABLE III
STATISTICAL ANALYSIS OF FALL DETECTION BY EACH FEATURE FOR DIFFERENT TYPES OF FALLS

Fall Number	Percentage of fall detection by each feature.			
	Imbalance	Imbalance Bump	Imbalance Bump Damping	Imbalance Bump Damping Recovery
1	100%	100%	100%	100%
2	100%	100%	100%	100%
3	100%	100%	100%	100%
4	100%	100%	100%	100%
5	100%	100%	100%	100%
6	100%	100%	100%	100%
7	100%	100%	100%	100%
8	100%	100%	100%	100%
9	100%	100%	100%	100%
10	100%	100%	100%	100%
11	100%	100%	100%	100%
12	100%	100%	100%	100%

collect more false alarms, we can optimize the thresholds better.

We use air mattress to simulate the ground. The real max g value will be smaller than the solid ground. That is why there still exists the false alarm. It is impossible to simulate the man fell using the real ground. In the beginning, we also push the solid doll into the ground. The behavior is also different with real man fell into the air mattress. On the other hand, many other researchers also use mattress to simulate the fall.

B. Physical Activity

We define a movement as the following.

$$SVM > 1g + p_2 \tag{12}$$

p_2 : the percent of $1g$ at approximately 10%.

Due to the physical characteristic, the SVM signal of the sensor will remain at baseline, 1g. If RB moves to the ground, the SVM will decrease. If you stop the descent to the ground, the SVM will increase due to inertia. We define the movement at higher side of 1 g. Next, we define a fixed time slot, during the subsequent 1 to 2 seconds. If we observe SVMs in a time slot and one SVM meets the criterion of Eq. (12), we define this time slot as a movement time slot while other time slots are defined as a motionless time slot. Due to real-time indoor position, the band will broadcast information every second. We accumulate movement data every 5 minutes and repeat the same movement information before next 5 minutes. The time slot is chosen every 2 seconds over 150 time slots, and the data are within one byte. Fig. 5 shows the examples of movement time slot.

Next, we define physical activity percentage. Physical activity percentage equals total movement time slot/total observed time slot. This value can be an observation over a short (5 minutes) or a long observation (24 hours).

C. Experiment

1) Fall Detection:

a) Simulated data: We recorded 12 different types of falls and 22 types of activities using the AiCare System. Each type was recorded with 3 repeats. Activities included hand swinging, sitting down on a chair (chair with/without armrests), standing up from a chair (chair with/without armrests), lying down on a bed, getting up from a bed, stepping up the stairs, stepping down the stairs, walking, rotating the hand, moving hand up and down with band in left and right hand which are shown in Table IV.

We use the same method to overlap the SVM of 22 activities. The result is shown in Fig. 6.

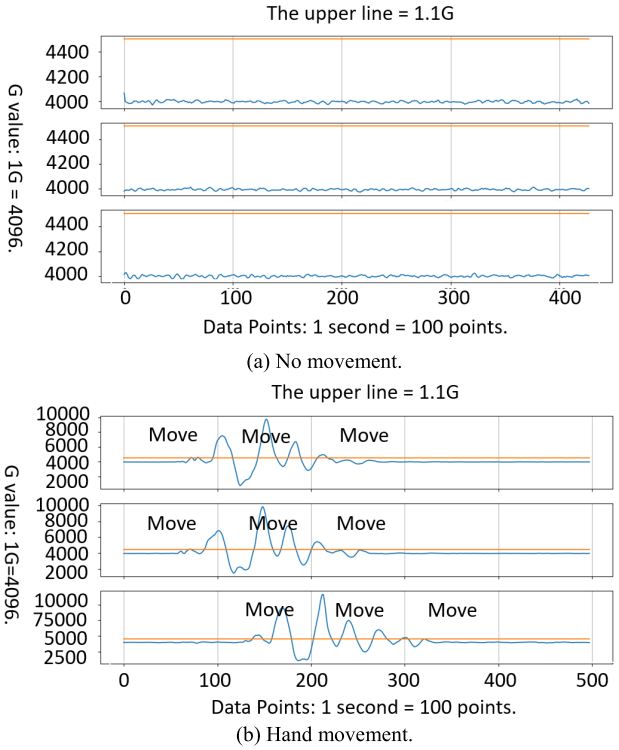

Fig. 5. Examples of movement time slot. (a) No movement. (b) Hand movement.

TABLE IV
TYPES OF ACTIVITIES

Number	Activity Type	Number	Activity Type
1	Hand swinging (left hand)	12	Hand swinging (right hand)
2	Sitting down on a chair (chair with armrests, left hand)	13	Sitting down on a chair (chair with armrests, right hand)
3	Sitting down on a chair (chair without armrests, left hand)	14	Sitting down on a chair (chair without armrests, right hand)
4	Standing up from a chair (chair with armrests, left hand)	15	Standing up from a chair (chair with armrests, right hand)
5	Standing up from a chair (chair without armrests, left hand)	16	Standing up from a chair (chair without armrests, right hand)
6	Lying down on a bed (left hand)	17	Lying down on a bed (right hand)
7	Getting up from a bed (left hand)	18	Getting up from a bed (right hand)
8	Stepping up the stairs (left hand)	19	Stepping up the stairs (right hand)
9	Stepping down the stairs (left hand)	20	Stepping down the stairs (right hand)
10	Walking (left hand)	21	Walking (right hand)
11	Rotating the hand (left hand)	22	Moving hand up and down (left hand)

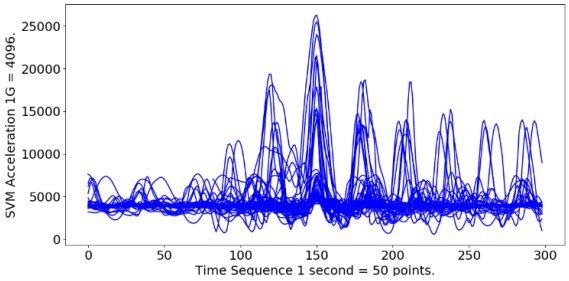

Fig. 6. The overlapped SVM of 22 activities.

TABLE V
STATISTICAL ANALYSIS OF FEATURE TEST IN DIFFERENT TYPES OF ACTIVITIES

Activity Number	Percentage of different activities with the features.			
	Imbalance	Imbalance Bump	Imbalance Bump Damping	Imbalance Bump Damping Recovery
1	100%	100%	66.67%	0%
2	33.33%	0%	0%	0%
3	66.67%	0%	0%	0%
4	66.67%	0%	0%	0%
5	33.33%	0%	0%	0%
6	0%	0%	0%	0%
7	33.33%	0%	0%	0%
8	100%	0%	0%	0%
9	100%	0%	0%	0%
10	100%	0%	0%	0%
11	100%	100%	0%	0%
12	100%	66.67%	66.67%	0%
13	0%	0%	0%	0%
14	66.67%	0%	0%	0%
15	66.67%	0%	0%	0%
16	33.33%	0%	0%	0%
17	0%	0%	0%	0%
18	66.67%	0%	0%	0%
19	100%	0%	0%	0%
20	100%	0%	0%	0%
21	100%	0%	0%	0%
22	100%	100%	100%	66.67%

Compared to Fig. 3, we saw the significant differences in all four phases of a fall: 1) increased evidence of imbalance 2) increased signal of bump 3) decreased damping, and 4) decreased recovery.

Table V shows the percentage of different types of activities has the features.

From the simulated data, we concluded the following results: 100% sensitivity (36/36), 96.88% specificity (64/[2 + 64]), 98.04% accuracy ([36 + 64]/[0 + 36 + 2 + 64]), 94.7% precision (36/[36 + 2]), 100% recall (36/[36 + 0]), and 97.3% F-measurement (with $\beta = 1$, [2 * 94.7%*100%]/[94.7% + 100%]). From Fig. 3 and Fig. 6, we observed significant difference between the 4 phases of a fall. And from Table VI, the statistical analysis shows that only 3.03% of non-fall activities will be recognized falsely as a fall using our features.

Furthermore, Table VII showed the increased in classification accuracy systemically for different feature combinations and feature fusion methods. The chi-square statistic was 80.5029, the p-value was < 0.00001 and the result was significant at $p < 0.05$. That rejected the equality of these 4 combinations of phases.

TABLE VI
THE CONFUSION MATRIX OF THE SIMULATED DATA

		True condition	
		Simulated fall	Activities
Predicted condition	Fall	36	2
	Non-fall	0	64

TABLE VII
THE ACCURACY OF THE COMBINATIONS OF PHASES

	Imbalance	Imbalance Bump	Imbalance Bump Damping	Imbalance Bump Damping Recovery
Accuracy	56.86%	89.22%	93.14%	98.04%

TABLE VIII
THE TRUTH TABLE OF THE SENIORS IN THE DAY CARE CENTER

		True condition	
		Fall	Non-fall
Predicted condition	Fall	2	1,187
	Non-fall	0	465,911

b) Day care center: Next, we used the same algorithm to assess the activities of the senior citizens at a day care center. The seniors went to day care center in the morning and return home in the evening. They wore the band at the day care center. They attended different classes, eat lunch and rest after lunch. Before they returned home in the late afternoon, the band is removed. There were 15 seniors and 3 assistants for this study. The average age was 79.9 ± 10.8 years old. We accumulated 519 person-day data in a total of 58 days; the maximum count of the seniors in one day was 15. The data from the assistants were 65 person-day in a total 25 days; the maximum count of the assistants in one day was 3. Table VIII shows the results of the seniors.

The data for 1189 falls were recorded by the AiCare System and 2 real falls were observed by the assistants. 465,911 was calculated from the following equation: the maximum fall counts were 519 (person-day) * 5.5 (hours / person-day) * 60 (minutes) * 60 (seconds) / 22 (seconds / fall) = 467,100 falls. 519 was total person-day. Each subject wore the band between 9:30 AM and 9:50 AM upon arrival to the day care center and took it off after 3:30 PM. We accumulated the data from 10:00 AM to 3:30 PM. The total hours were 5.5 hours. The time to judge a fall was 22 seconds. Next, 1187 and 2 were subtracted from 467,100, which equals 465,911 for the non-fall counts. From Table VIII, we concluded the following results: 100% sensitivity (2/2), 99.75% specificity (465,911 / [465,911 + 1,187]), 99.75% accuracy ([2 + 465,911] / [0 + 2 + 1,187 + 465,911]), 0.17% precision (2/[2 + 1187]), 100% recall (2/[2+0]), and 0.34% F-measurement (with $\beta = 1$, [2 * 0.17%*100%]/[0.17% + 100%]). The three assistants were also added for this analysis.

The total data was 65 person-day in 25 days. No fall was found in real condition. The data for 413 falls was recorded by the AiCare System and 0 real fall was observed by the assistants. The maximum fall counts were 65 (person-day) *

TABLE IX
THE CONFUSION MATRIX OF THREE ASSISTANTS IN THE DAY CARE CENTER

		True condition	
		Fall	Non-fall
Predicted condition	Fall	0	413
	Non-fall	0	58,087

TABLE X
THE DOSES OF QUETIAPINE FOR DIFFERENT SENIORS

ID	The dose of Quetiapine
Senior 1	225 mg/day
Senior 2	25 mg/day
Senior 3	0 mg/day
Senior 4	0 mg/day

5.5 (hours / person-day) * 60 (minutes) * 60 (seconds) / 22 (seconds / fall) = 58,500 falls. We achieved the following results: sensitivity was not available (0/0); specificity was 99.29% (58,087 / [413 + 58,087]); accuracy was 99.29% ([0 + 58,087]/[0 + 0 + 413 + 58,087]); precision was 0% (0/[0 + 413]); recall was not available; and F-measurement was not available.

2) Physical Activity: After we defined the movement time slot, we obtained the movement data every 5 minutes. We measured the activity data by dividing the activity count by 150 to be physical activity percentage for every 5 minutes. This represented the percentage of time when each person was in activity movement. The day care center rested after lunch from 12:00 PM to 13:30 PM. During this time, every senior remained in a chair bed. We divided the day hours into class and rest hours. The class hours were spent with the teachers and assistants. The lunch nap was considered as rest hours.

We also measured the physical activity of the seniors with dementia, requiring anti-psychotic medication. Some level of dementia was a common disease among the seniors. Some seniors had delusion during the early and middle stages of the disease process, impeding their sleep at night. If they had this condition, they are prescribed Quetiapine [29], which was primarily used to treat schizophrenia or bipolar disorder as a mood stabilizer. One of the common major side effects was decreased physical activity [25]. We proceeded to assess if our defined physical activity percentage can distinguish the behavior differences of those taking increasing doses of Quetiapine. In our study, there were four seniors with dementia taking Quetiapine. They were taking 3 different doses of Quetiapine as shown in Table X.

We checked the physical activity percentage (a day per data point) of these four seniors. The results are in Fig. 7.

Next, we studied the data using box plot. The results are shown in Fig. 8 and Table XI shows means and standard deviations.

We then observed for a longer period, and the data were validated by assistants who visually confirmed the activity level for reference. The results are shown in Fig. 9 and 10. Table XII shows means and standard deviations.

Next, we measured the physical activity percentage (5 minutes per data point) during the day.

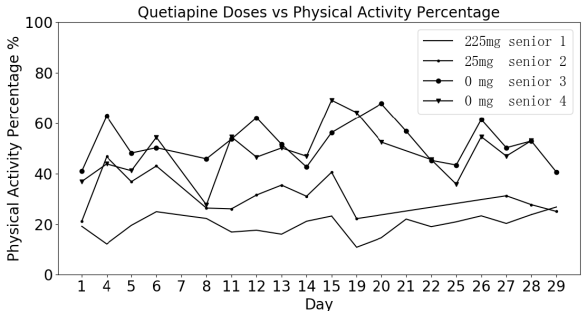

Fig. 7. One month data of physical activity (a day per data point) percentage in different doses of Quetiapine.

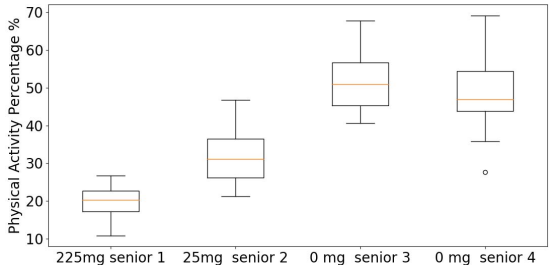

Fig. 8. The box plot of physical activity percentage (a day per data point).

TABLE XI
THE MEAN AND STANDARD DEVIATIONS OF PHYSICAL ACTIVITY PERCENTAGE

ID	Mean	Standard Deviations
Senior 1	19.71%	4.23%
Senior 2	31.76%	7.81%
Senior 3	51.77%	8.12%
Senior 4	48.41%	10.13%

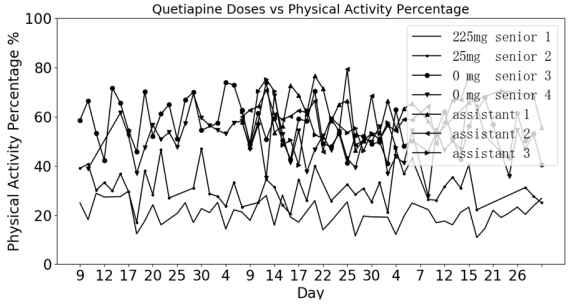

Fig. 9. Three-month data of physical activity percentage (a day per data point) in different doses of Quetiapine and validated by the 3 assistants.

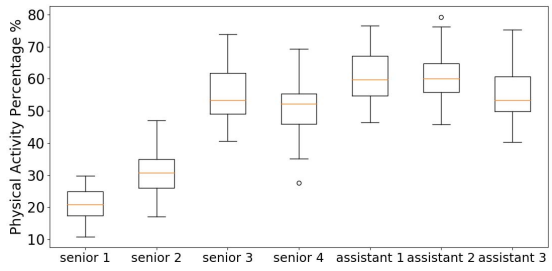

Fig. 10. The box plot of physical activity percentage (a day per data point) over 3 months including the 3 assistants.

The observed data confirmed that the seniors rested in a reclining chair bed from 12:00 PM to 1:30 PM. The physical activity percentage decreased significantly during this period

TABLE XII
THE MEAN AND STANDARD DEVIATIONS OF PHYSICAL ACTIVITY PERCENTAGE

ID	Mean	Standard Deviations
Senior 1	20.76%	4.92%
Senior 2	31.25%	7.14%
Senior 3	56.06%	9.17%
Senior 4	50.46%	8.73%
Assistant 1	61.15%	8.16%
Assistant 2	60.47%	7.85%
Assistant 3	55.61%	9.12%

TABLE XIII
THE AVERAGE PHYSICAL ACTIVITY PERCENTAGE OF THE CLASS AND THE NAP

ID	The Class (10:00 AM to 12:00 PM and 1:30 PM to 3:30 PM)	The Nap (12:00 PM to 1:30 PM)
Senior 1	20.15%	6.95%
Senior 2	30.54%	11.08%
Senior 3	51.66%	12.45%
Senior 4	41.94%	12.50%

(Table XIII). We also observed that Assistant 3 rested from 12:45 PM to 1:30 PM. These three assistants ate lunch from 12:00 PM. After lunch, Assistants 1 and 2 did arts and crafts and Assistant 3 rested. We then generated a detailed normalized histogram (the sum of the histogram is normalized to 1) for them. Fig. 12 shows a normalized histogram of Fig. 10 removing the napping data from 12:00 PM to 1:30 PM. We observed that there is a high bar at $x = 0$.

III. DISCUSSION

A. Fall Detection

First, we simulated the falls and recorded the data. We considered the resources and removed the initial conditional difference (wore sensor on the left or right wrist and rotated the position). We used SVM for our fall detection parameter and introduce a pattern recognition method for fall detection. Our simulated data were training data sets and the day care center data were the test data sets. We achieved a highly reliable result using simulated data (100% sensitivity, 96.88% specificity, 98.04% accuracy, 94.7% precision, 100% recall, and 97.3% F-measurement). Next, we used the same algorithm for 584 person-day and total during for about 3 months. We separated the subjects into two groups: the seniors ($n = 15$, 79.9 ± 10.8 years old) and the youths (Assistants 1-3, $n = 3$, 21.7 ± 0.6 years old). A real fall was a very low-frequency event. There were 2 senior falls with no injury. Our algorithm for the seniors demonstrated 100% sensitivity, 99.75% specificity, 99.75% accuracy, 0.17% precision, 100% recall, and 0.34% F-measurement. We saw precision and F-measurement drop when compared to the simulated vs. real condition. The main reason was that real falls are infrequent and if the algorithm had false positive, this translates to less precision and F-measurement. If no real falls happened, the precision was always 0. From the senior data, the algorithm demonstrated 2.3 false alarms during the day and one false alarm in 2.4 (= 5.5/2.3) hours (in the night, the false alarm was less). The youth data showed 99.29% specificity, 99.29% accuracy, 0% precision, no recall, and no F-measurement. The algorithm for the youths demonstrated 6.4 false alarms during the day and one false alarm in 0.87 (= 5.5/6.4) hour. There was a reduction in specificity and accuracy for the youths (compared to loss from 100%, the youth assistants were triple of the seniors $-0.71/-0.25 = 2.84$). From Tables VIII (the seniors) and 9 (the young assistants), we concluded that our proposed algorithm was more suitable for the seniors, because their falls tend to be quicker, generating higher g-value activity. If the seniors demonstrated a fall-like activity based on the higher g-value, there was a higher likelihood of indicating a fall. The younger cohorts could easily perform a fall-like activity and generate higher g-value without falling, resulting in higher false positive alarms.

Our algorithm was based on the fall pattern recognition (4 phases), using state machine method. If there was a fall, the subject might be conscious or unconscious. If they could still move, they could use alert service for help. If they were unconscious, we used a pre-specified period with zero physical activity to detect and confirm the fall. Our limitations included the following: 1) false alarms still existed and 2) the younger cohort performed higher g-value activity, which simulated a fall.

Ahmad and Khan [21] detect the following activity recognitions: walking, walking up-stairs, walking down-stairs, running, and jogging which are interesting but different from our fall detection.

Mathews *et al.* [32]–[34] proposed a series of methods about dictionary learning. They used dictionary pair learning based on maximum correntropy criterion (more insensitive to outliers) and a class specific regularizer term (better classification). They differentiated more activities, using 3 IMU sensors in different positions. Compared to our application: 1) activities did not include falls, 2) accuracy decreased when using only one IMU sensor, 3) matrix multipliers required higher power consumption, 4) more data were necessary for user independent measurements, and 5) 100% sensitivity must be maintained.

Wang *et al.* [15] explained many important topics regarding deep learning on sensor-based human activity recognition. Mathews [30] proposed a real-time activity recognition using convolutional neural networks. They recognized 6 different activities using accelerometer data from smartphone. Our band did not perform CNN calculations. If we do upgrade our band to perform CNN, the band cannot be used over 45 days due to significant power consumption issue.

Lee *et al.* [31] introduced explainable artificial intelligence in the following applications: NLP, biomedical, and malware classification. The basic problem of misclassified samples was our features could not distinguish the real fall and fall like activity. We need more features to separate them.

Our selected features were small pieces of motion. The sequences of these features composed a fall or fall-like activity. These features were hand-crafted. We used an automatic feature selection approach if we had enough dataset from many

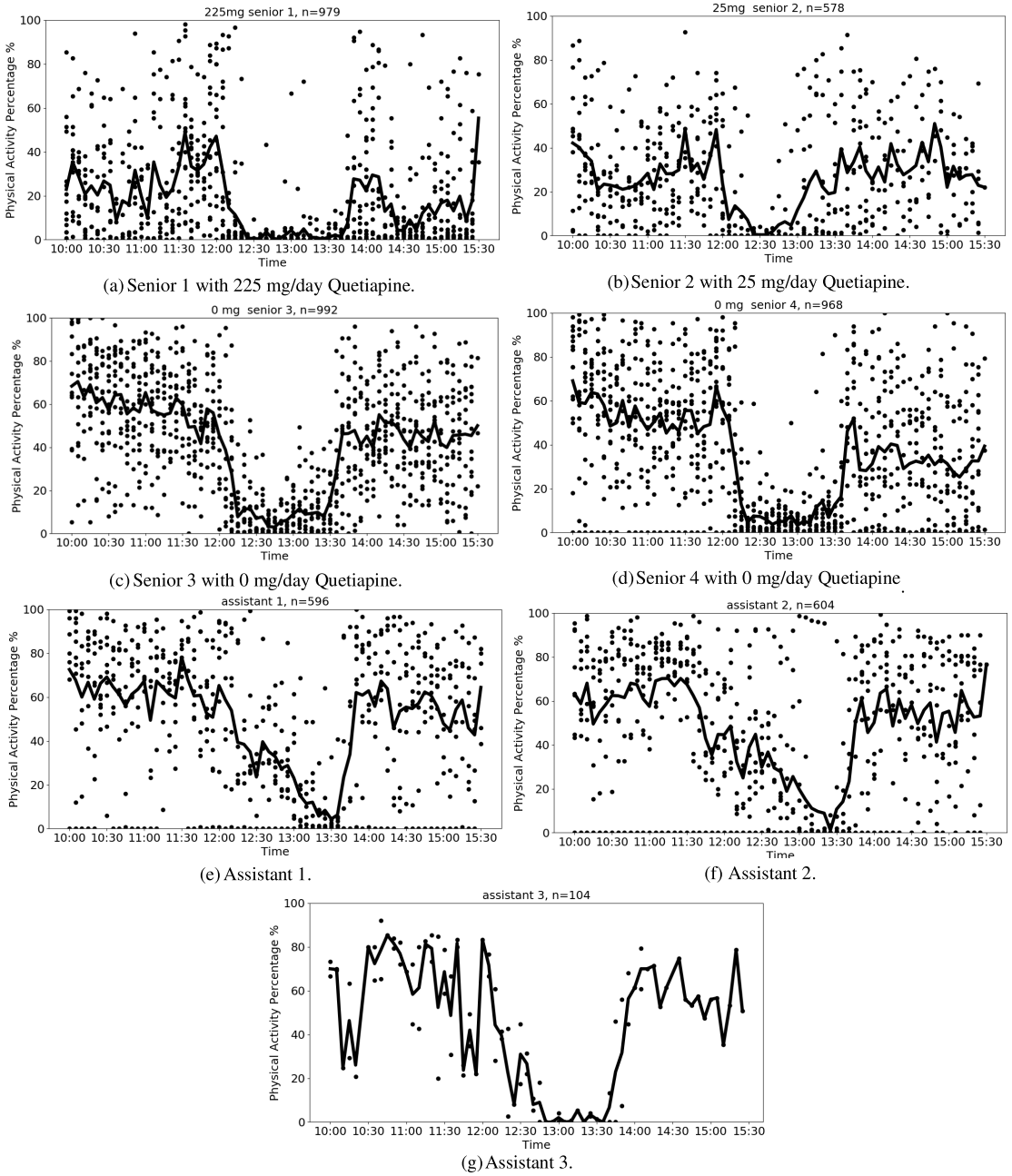

Fig. 11. Physical activity percentage (5 minutes per data point) with time. Solid lines are the averages of each time slot.

subjects who sustain a fall. On the other hand, the machine feature selection method required many more features to calculate in order to detect a fall. This requirement would not allow our band to maintain power over 45 days.

B. Physical Activity

Using our proposed method, physical activity percentage was measured to assess physical activity. We then proceeded to assess whether the algorithm can distinguish the behavior of the seniors taking different doses of Quetiapine. The senior with highest dose of Quetiapine demonstrated lowest level of physical activity percentage (19.71% in Table XI and 20.76% in Table XII). We found that Senior 3 and Assistant 3 (56.06% vs 55.61%, $p > 0.05$) and Assistants 1 and 2 (61.15% vs 60.47%, $p > 0.05$) also had similar level of the physical activity percentage. Since the assistants coached the seniors, their physical activity percentage should be similar to the seniors who participated in the class but within individual physical limitations. There were many reasons why the physical activity percentage varied. The reasons could not be attributed only to the dose difference. Ideally, we preferred to monitor the physical activity percentage with different doses in the same person or increase the sample size. Baseline activity level prior to their starting the medication should be obtained.

From Fig. 11(a), (c), and (d), we clearly knew that the seniors rest from 12:00 PM to 1:30 PM. The pattern of one month data also indicated the physical activity percentage of the senior citizens. The seniors with high physical activity

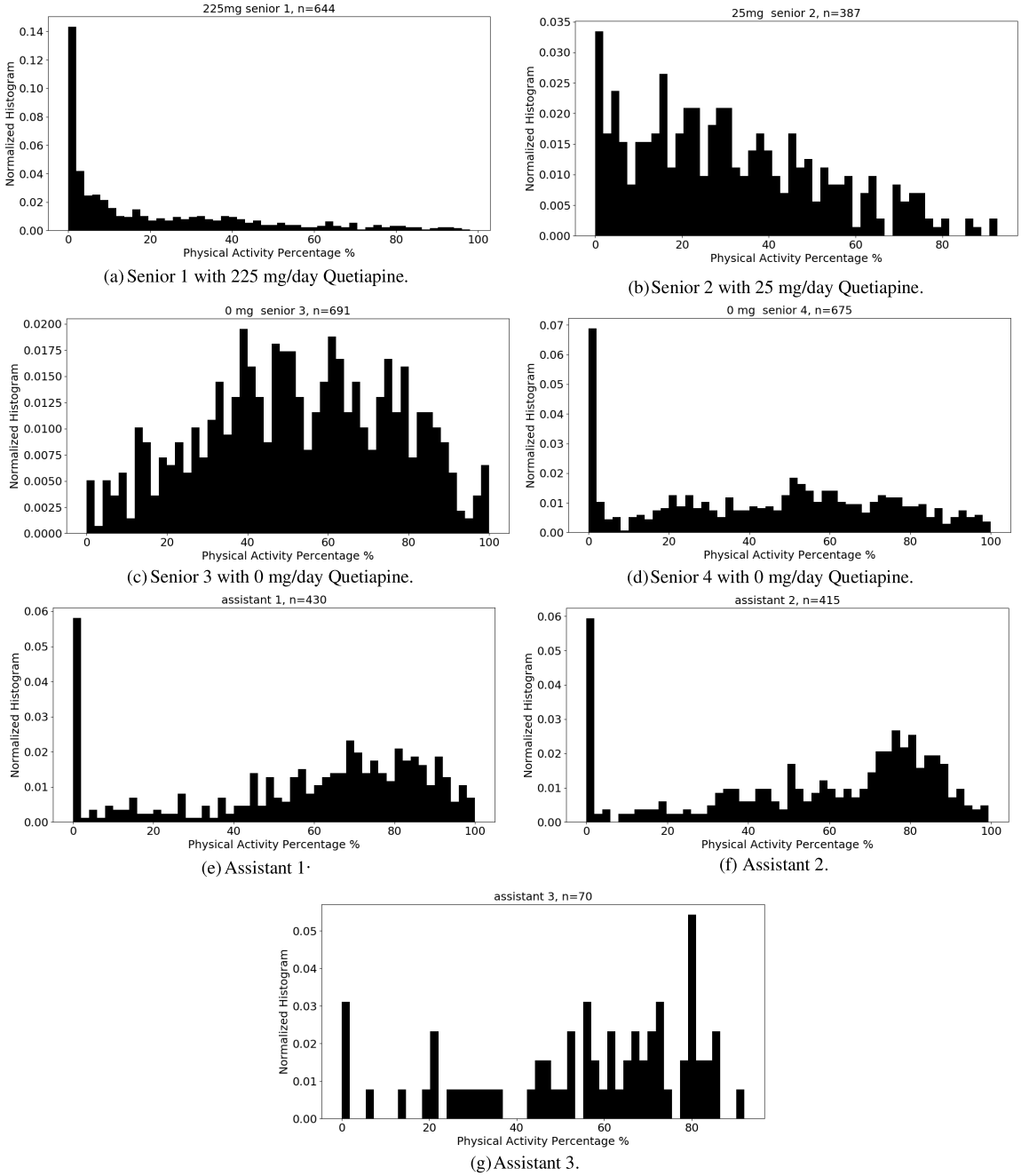

Fig. 12. Normalized histogram for the senior citizens (1-4) and assistants (1-3).

percentage will have more points in upper region (from the definition of y-axis). It recorded the senior's physical activity percentage pattern. We used the pattern data to check if they had changed during the month. We also employed the pattern data to classify the group of the seniors.

Fig. 11 shows the activity tracking of each subject over one-month period. The tracking demonstrated each subject with a unique activity pattern. We used this footprint to track each month to know the activity trend of each subject. We also categorized these footprints into different groups by unsupervised learning and data clustering algorithms. We knew the characteristics of each group, which correspond to optimized lifestyle for each group or each subject. These findings demonstrated the unique ability to delineate the activity for each subject, emphasizing the importance to personalize the data for each subject. AiCare is employing artificial intelligence such as machine learning to assist in detecting and understanding the individual activity difference.

The normalized histogram generated interesting data. Fig. 12 (c) and (g) demonstrated different patterns compared to (a), (b), (d), (e), and (f). Fig. 12 (a), (b), (d), (e), and (f) showed that they have the most percentage in the zero zone (14.34%, 3.35%, 6.89%, 5.81%, and 5.94%) while (g) exhibited insufficient data ($n = 70$) and indicated different pattern. The data represented the highest similar physical activity percentage in the zero zone (rest). This finding was reasonable

since senior citizens rest when they were able to do so. From zero zone percentage, we also knew the reasonable value for each subject. If a subject exhibited small value in zero zone (for example: 0%), we would know why it was abnormal. It may be the early stage of the disorder. But this designation would require more data to infer this finding.

IV. Conclusion

In this study, we demonstrated the requirements to detect falls and assess physical activities for the seniors, employing RB from the AiCare System. We propose two IMU applications, high impact detection and physical activity level measurement. Our main contribution for fall detection used pattern recognition method by state machine detection. It demonstrated high sensitivity, specificity, and accuracy. Low-power consumption was possible by only using triaxial accelerometer. While false positive alarm still existed, this algorithm was most effective for the activity level of the seniors.

We used state machine method to detect a fall and we defined four phases to detect a fall with higher accuracy and fewer false alarms. No one used the same method before. On the other hand, our system also used alert service and physical activity to help fall detection.

For physical activity, we proposed a method to distinguish the different level of physical activities. Specifically, the effects of medication and the different doses were distinguished. We thought our proposed method could be a good tool to assess the baseline physical activity level and the subsequent changes in activity level. Furthermore, our proposed method also allowed fall detection. If the subjects were conscious, they were able to press the button to activate the alert service. If they were unconscious or immobile, we could use zero physical activity percentage for a pre-determined duration to confirm a fall after a high impact motion.

Our system aimed to help the nursing care infrastructures to have better tools for easier management. We tried these technologies to help the seniors and the senior care infrastructures.

References

[1] Administration for Community Living. (2017). *Profile of older Americans*. [Online]. Available: https://acl.gov/aging-and-disability-in-america/data-and-research/profile-older-americans,

[2] A. Sorvala, E. Alasaarela, H. Sorvoja, and R. Myllyla, "A two-threshold fall detection algorithm for reducing false alarms," in *Proc. 6th Int. Symp. Med. Inf. Commun. Technol. (ISMICT)*, La Jolla, CA, USA, Mar. 2012, pp. 1–4.

[3] B. G. Steele, L. Holt, B. Belza, S. Ferris, S. Lakshminaryan, and D. M. Buchner, "Quantitating physical activity in COPD using a triaxial accelerometer," *Chest*, vol. 117, no. 5, pp. 1359–1367, May 2000.

[4] C. A. Werner. (2010). *The Older Population: 2010, Census Briefs U.S. Bureau of the Census*. [Online]. Available: http://www.census.gov/prod/cen2010/briefs/c2010br-09.pdf

[5] C. C. Yang and Y. L. Hsu, "Development of a portable system for physical activity assessment in a home environment," in *Proc. Int. Comput. Symp.*, Taiwan, Japan, 2006, pp. 45–50.

[6] Centers for Disease Control and Prevention. (2018). *Home and Recreational Safety*. [Online]. Available: https://www.cdc.gov/homeandrecreationalsafety/falls/adultfalls.html

[7] C. J. Caspersen, K. E. Powell, and G. M. Christenson, "Physical activity, exercise and physical fitness: Definitions and distinctions for health-related research," *Public Health Rep.*, vol. 110, pp. 126–131, Oct. 1985.

[8] C.-C. Wang *et al.*, "Development of a fall detecting system for the elderly residents," in *Proc. 2nd Int. Conf. Bioinf. Biomed. Eng.*, Shanghaim, China, May 2008, pp. 1359–1362.

[9] D. E. O'Leary, "Artificial intelligence and big data," *IEEE Intell. Syst.*, vol. 28, no. 2, pp. 96–99, Mar. 2013, doi: 10.1109/MIS.2013.39.

[10] D. Lim, C. Park, N. H. Kim, S.-H. Kim, and Y. S. Yu, "Fall-detection algorithm using 3-Axis acceleration: Combination with simple threshold and hidden Markov model," *J. Appl. Math.*, vol. 2014, Jan. 2014. Art. no. 896030.

[11] E. Casilari, J. A. Santoyo-Ramón, and J. M. Cano-García, "UMAFall: A multisensor dataset for the research on automatic fall detection," *Procedia Comput. Sci.*, vol. 110, pp. 32–39, Feb. 2017.

[12] F. Gemperle, C. Kasabach, J. Stivoric, M. Bauer, and R. Martin, "Design for wearability," in *Proc. 2nd Int. Symp. Wearable Comput.*, Pittsburg, CA, USA, 1998, pp. 116–122.

[13] F. Hossain, M. L. Ali, M. Z. Islam, and H. Mustafa, "A direction-sensitive fall detection system using single 3D accelerometer and learning classifier," in *Proc. Int. Conf. Med. Eng., Health Informat. Technol. (MediTec)*, Dhaka, Bangladesh, Dec. 2016, pp. 1–6.

[14] G. Vavoulas, M. Pediaditis, E. G. Spanakis, and M. Tsiknakis, "The MobiFall dataset: An initial evaluation of fall detection algorithms using smartphones," in *Proc. 13th IEEE Int. Conf. Bioinf. BioEng.*, Greece, China, Nov. 2013, pp. 1–4.

[15] J. Wang, Y. Chen, S. Hao, X. Peng, and H. Lisha, "Deep learning for sensor-based activity recognition: A survey," *Pattern Recognit. Lett.*, vol. 119, pp. 3–11, Mar. 2019, doi: 10.1016/j.patrec.2018.02.010.

[16] J. Zakir, T. Seymour, and K. Berg, "Big data analytics," *Issues Inf. Syst.*, vol. 16, no. 2, pp. 81–90, 2015.

[17] K. M. Diaz *et al.*, "Fitbit: An accurate and reliable device for wireless physical activity tracking," *Int. J. Cardiol.*, vol. 185, pp. 138–140, Apr. 2015.

[18] L. Hutchison, C. Hawes, and L. Williams, "Access to quality health service in rural areas-long-term care," in *Rural Healthy People 2010: A Companion Document to Healthy People*, vol. 3. College Station, TX, USA: Southwest Rural Health Research Center, 2010.

[19] L. Zhu *et al.*, "A survey of fall detection algorithm for elderly health monitoring," in *Proc. IEEE 5th Int. Conf. Big Data Cloud Comput.*, Dalian, China, Aug. 2015, pp. 270–274.

[20] M. Ahmad, A. M. Khan, J. A. Brown, S. Protasov, and A. M. Khattak, "Gait fingerprinting-based user identification on smartphones," in *Proc. Int. Joint Conf. Neural Netw. (IJCNN)*, Vancouver, BC, Canada, Jul. 2016, pp. 3060–3067, doi: 10.1109/IJCNN.2016.7727588.

[21] M. Ahmad and A. M. Khan, "Seeking optimum system settings for physical activity recognition on smartwatches," in *CoRR*, vol. abs/1706.01720. Ithaca, NY, USA: Cornell Univ. Library, 2017.

[22] M. Ahmad, A. M. Khan, M. Mazzara, S. Distefano, A. Ali, and A. Tufail, "Extended sammon projection and wavelet kernel extreme learning machine for gait-based legitimate user identification," in *Proc. 34th ACM/SIGAPP Symp. Appl. Comput.*, Apr. 2019, pp. 1216–1219.

[23] M. E. Rida, F. Liu, Y. Jadi, A. A. A. Algawhari, and A. Askourih, "Indoor location position based on Bluetooth signal strength," in *Proc. 2nd Int. Conf. Inf. Sci. Control Eng.*, Shanghai, China, Apr. 2015, pp. 769–773.

[24] P. Pierleoni, A. Belli, L. Palma, M. Pellegrini, L. Pernini, and S. Valenti, "A high reliability wearable device for elderly fall detection," *IEEE Sensors J.*, vol. 15, no. 8, pp. 4544–4553, Aug. 2015.

[25] P. Vallabh, R. Malekian, N. Ye, and D. C. Bogatinoska, "Fall detection using machine learning algorithms," in *Proc. 24th Int. Conf. Softw., Telecommun. Comput. Netw. (SoftCOM)*, Split, India, Sep. 2016, pp. 1–9.

[26] S. Khojasteh, J. Villar, C. Chira, V. González, and E. de la Cal, "Improving fall detection using an on-wrist wearable accelerometer," *Sensors*, vol. 18, no. 5, p. 1350, Apr. 2018, doi: 10.3390/s18051350.

[27] S. Kajioka, T. Mori, T. Uchiya, I. Takumi, and H. Matsuo, "Experiment of indoor position presumption based on RSSI of Bluetooth LE beacon," in *Proc. IEEE 3rd Global Conf. Consum. Electron. (GCCE)*, Tokyo, Japan, Oct. 2014, pp. 337–339.

[28] S. F. Hossain, M. Z. Islam, and M. L. Ali, "Real time direction-sensitive fall detection system using accelerometer and learning classifier," in *Proc. 4th Int. Conf. Adv. Electr. Eng. (ICAEE)*, Dhaka, Bangladesh, Sep. 2017, pp. 99–104.

[29] S. M. Cheer and A. J. Wagstaff, "Quetiapine. A review of its use in the management of schizophrenia," *CNS Drugs*, vol. 18 no. 3, pp. 173–199, 2004.

[30] S. M. Mathews, "Explainable artificial intelligence applications in NLP, biomedical, and malware classification: A literature review," in *Proc. Comput. Conf.*, 2019, pp. 1269–1292, doi: 10.1007/978-3-030-22868-2_90.

[31] S.-M. Lee, S. Min Yoon, and H. Cho, "Human activity recognition from accelerometer data using convolutional neural network," in *Proc. IEEE Int. Conf. Big Data Smart Comput. (BigComp)*, Seoul, South Korea, Feb. 2017, pp. 131–134, doi: 10.1109/BIGCOMP.2017.7881728.

[32] S. M. Mathews, C. Kambhamettu, and K. E. Barner, "Maximum correntropy based dictionary learning framework for physical activity recognition using wearable sensors," in *Proc. 12th Int. Symp. Vis. Comput. (ISVC)*, Las Vegas, NV, USA, 2016, Art. no. 10073, doi: 10.1007/978-3-319-50832-0_13.

[33] S. M. Mathews, C. Kambhamettu, and K. E. Barner, "Centralized class specific dictionary learning for wearable sensors based physical activity recognition," in *Proc. 51st Annu. Conf. Inf. Sci. Syst. (CISS)*, Baltimore, MD, USA, Mar. 2017, pp. 1–6.

[34] S. M. Mathews, C. Kambhamettu, and K. E. Barner. (2017). *Dictionary and Deep Learning Algorithms With Applications to Remote Health Monitoring Systems*. [Online]. Available: http://udspace.udel.edu/handle/19716/21241

[35] T. Mauldin, M. Canby, V. Metsis, A. Ngu, and C. Rivera, "SmartFall: A smartwatch-based fall detection system using deep learning," *Sensors*, vol. 18, no. 10, p. 3363, Oct. 2018, doi: 10.3390/s18103363.

[36] U. Lindemann, A. Hock, M. Stuber, W. Keck, and C. Becker, "Evaluation of a fall detector based on accelerometers: A pilot study," *Med. Biol. Eng. Comput.*, vol. 43, pp. 1146–1154, Feb. 2005.

[37] X. Wu *et al.*, "Top 10 algorithms in data mining," *Knowl. Inf. Syst.*, vol. 14, no. 1, pp. 1–37, Jan. 2008, doi: 10.1007/s10115-007-0114-2.

[38] Z. Jianyong, L. Haiyong, C. Zili, and L. Zhaohui, "RSSI based Bluetooth low energy indoor positioning," in *Proc. Int. Conf. Indoor Positioning Indoor Navigat. (IPIN)*, Busan, South Korea, Oct. 2014, pp. 526–533.

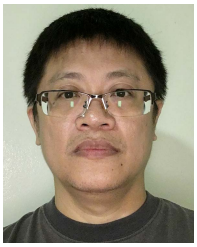

Hung-Ping Liu received the B.S. degree in computer science and information engineering from National Chiao Tung University, Hsinchu, Taiwan, in 1994, and the M.S. degree in computer science and information engineering and the Ph.D. degree in biomedical electronics and bioinformatics from National Taiwan University, Taipei, Taiwan, in 1996 and 2019, respectively. His research interests include computer vision, pattern recognition, and machine learning.

Yu-Min Chuang received the B.S. degree in medicine and the Ph.D. degree in biomedical imaging from National Yang-Ming University, Taipei, Taiwan, in 1997 and 2009, respectively. His research interests include cerebrovascular disease, medical imaging, and leprosy.

Chih-Hao Liu received the M.S. degree in electrical engineering from the National Taiwan University of Science and Technology, Taipei, Taiwan, in 2001, and the Ph.D. degree in applied mechanics from National Taiwan University, Taipei, in 2012. His research interests include medical device, the AIoT, nanomechanics, and healthcare robot.

Phillip C. Yang received the B.A.S. and M.A. degrees from Stanford University and the M.D. degree from the Yale University School of Medicine. He completed a post-graduate training at UCLA and Stanford University Medical Centers. He is a physician-scientist. His research interests include clinical translation of novel molecular/cellular processes of myocardial restoration and application of related multiomic data through deep learning and artificial intelligence. He is an Associate Professor at Stanford University and a Co-Founder of AiCare, Inc. He leads multiple research projects funded by national agencies such NIH and AHA. He was a recipient of several prestigious awards, including the NIH Career Development Award, the NIH Career Enhancement Award, and the NIH Patient Oriented Research.

Chiou-Shann Fuh (Member, IEEE) received the B.S. degree in computer science and information engineering from National Taiwan University, Taipei, Taiwan, in 1983, the M.S. degree in computer science from Pennsylvania State University, University Park, PA, in 1987, and the Ph.D. degree in computer science from Harvard University, Cambridge, MA, in 1992. He was with AT&T Bell Laboratories and engaged in performance monitoring of switching networks from 1992 to 1993. He was an Associate Professor with the Department of Computer Science and Information Engineering, National Taiwan University, from 1993 to 2000, where he was promoted to a Full Professor. His current research interests include digital image processing, computer vision, pattern recognition, mathematical morphology, deep learning, artificial intelligence, and their applications to defect inspection, industrial automation, digital still camera, digital video camcorder, surveillance camera, and camera module, such as color interpolation, auto exposure, auto focus, auto white balance, color calibration, and color management.